PR130 is a modulator of the Wnt-signaling cascade that counters repression of the antagonist Naked cuticle

Menno P. Creyghton*†, Giulietta Roël†‡, Pieter J. A. Eichhorn*, Liesbeth C. Vredeveld*, Olivier Destrée‡, and René Bernards*§

*Division of Molecular Carcinogenesis and Center for Biomedical Genetics, Netherlands Cancer Institute, Plesmanlaan 121, 1066 CX, Amsterdam, The Netherlands; and ‡Netherlands Institute for Developmental Biology (NIOB), Hubrecht Laboratory, Uppsalalaan 8, 3584 CT, Utrecht, The Netherlands

Edited by Roel Nusse, Howard Hughes Medical Institute, Stanford, CA, and accepted by the Editorial Board March 1, 2006 (received for review December 16, 2005)

The Wnt-signaling cascade is required for several crucial steps during early embryogenesis, and its activity is modulated by various agonists and antagonists to provide spatiotemporal-specific signaling. Naked cuticle is a Wnt antagonist that itself is induced by Wnt signaling to keep Wnt signaling in check. Little is known about the regulation of this antagonist. We have recently shown that the protein phosphatase 2A regulatory subunit PR72 is required for the inhibitory effect of Naked cuticle on Wnt signaling. In the present study, we show that PR130, which has an N terminus that differs from that of PR72 but shares the same C terminus, also interacts with Naked cuticle but instead functions as an activator of the Wnt-signaling pathway, both in cell culture and during development. We find that PR130 modulates Wnt signal transduction by restricting the ability of Naked cuticle to function as a Wnt inhibitor. Our data establish PR130 as a modulator of the Wnt-signaling pathway and suggest a mechanism of Wnt signal regulation in which the inhibitory activity of Naked cuticle is determined by the relative level of expression of two transcripts of the same protein phosphatase 2A regulatory subunit.

development | protein phosphatase 2A | *Xenopus*

Increasing molecular data now describe in impressive detail the different specialized steps involved in the evolution of a complex organism from a single fertilized cell. A surprisingly small number of signaling routes is responsible for the critical steps required to undergo the major developmental changes during early embryogenesis (1–4). The Wnt-signaling pathway is required for several essential developmental processes, such as body axis specification, segmentation, and gastrulation movements. Activation of this pathway is initiated by binding of Wnt ligands to the seven-pass transmembrane receptor frizzled and the coreceptors LRP5/6. Several Wnt ligands have been identified that can activate distinct classes of Wnt-dependent signaling routes, resulting in distinct developmental fates (for review, see ref. 5). Activation of the frizzled receptor signals to dishevelled, which functions as a docking platform for other components of the Wnt cascade and is required for signaling through the different Wnt-mediated pathways (6, 7).

The canonical pathway is involved in specifying the dorso/ventral body axis and segmentation of the embryo (5). During canonical Wnt signaling, Wnt ligand binding to the receptor initiates a signal that is passed through dishevelled to disrupt the Axin/APC/GSK3β complex. This so-called β-catenin destruction complex facilitates the sequential phosphorylation of the protooncogene β-catenin by the CK1 and GSK3β protein kinases (8). This phosphorylation targets β-catenin for degradation by the proteasome. When the destruction complex is disabled, β-catenin can accumulate and enter the nucleus where it binds to the T cell factor (TCF) family of transcription factors. This interaction then leads to the transcription of Wnt target genes (9). Not surprisingly, mutations affecting the activity of the canonical Wnt pathway in adult tissues are causally involved in oncogenic transformation (10, 11), emphasizing the continuous requirement of correct control over this pathway. During development, it is essential that active Wnt signaling is restricted both temporally and spatially. This restriction is accomplished by the induction of antagonists such as axin2/conductin (12, 13) and Naked cuticle (Nkd) (14), which are both transcriptional targets of the Wnt pathway. Nkd was initially found in *Drosophila* to be required for the establishment of segment polarity by antagonizing Wingless (Wg) activity (14). *Drosophila nkd* mutants lack denticles, as seen in embryos exposed to excess Wg (15). This function of Nkd is evolutionarily conserved, as was demonstrated for mouse Nkd1 (mNkd1) and mNkd2, which can both antagonize the Wnt-signaling pathway in Wnt reporter assays (16). Ectopic expression of mNkd1 in *Drosophila* inhibits Wg activity (16). In vertebrates, Nkd is expressed in several tissues during development, such as the dorsal CNS, the somites, forelimbs, and tailbud (16). At the molecular level, Nkd interacts with, and functions as an inhibitor at the level or upstream of, dishevelled (16–18). In addition, we have previously shown that Nkd can influence the stability of dishevelled at the protein level (19). We also identified PR72 as a modulator of the Wnt-signaling pathway through its interaction with Nkd and found that PR72 is required for the inhibitory function of Nkd during embryonic development. We now report that Nkd interacts with PR130, a PR72-related protein phosphatase type 2A (PP2A) regulatory B-subunit having a distinct N terminus (20). We show that endogenous PR130 functions as an activator of the pathway and that Nkd can no longer antagonize Wnt signaling in the presence of excess PR130. Furthermore, PR130 seems to oppose the action of PR72. This finding establishes PR130 as a Wnt modulator and describes a way to fine-tune the Wnt signal.

Results

PR130 Interacts with Nkd and Recruits the PP2A Complex. PR130 was described earlier as the larger variant of PR72 (20) containing a stretch of 665 aa specific for this protein at the N terminus, replacing the 44 specific N-terminal amino acids for PR72 (Fig. 1*A*). Both proteins are conserved among vertebrates and are generated by transcription from distinct promoters (20). Because PR72 has only 44 N-terminal amino acids that are specific to PR72, whereas the remaining 483 aa are 100% identical between these two proteins,

Conflict of interest statement: No conflicts declared.

This paper was submitted directly (Track II) to the PNAS office. R.N. is a guest editor invited by the Editorial Board.

Freely available online through the PNAS open access option.

Abbreviations: IP, immunoprecipitation; HA, hemagglutinin; HEK, human embryonic kidney; PP2A, protein phosphatase type 2A; TCF, T cell factor; MO, morpholino oligonucleotide; Nkd, Naked cuticle; Xnkd, *Xenopus* Nkd; hNkd, human Naked; ISH, *in situ* hybridization; QRT-PCR, quantitative RT-RCR.

†M.P.C. and G.R. contributed equally to this work.

§To whom correspondence should be addressed. E-mail: r.bernards@nki.nl.

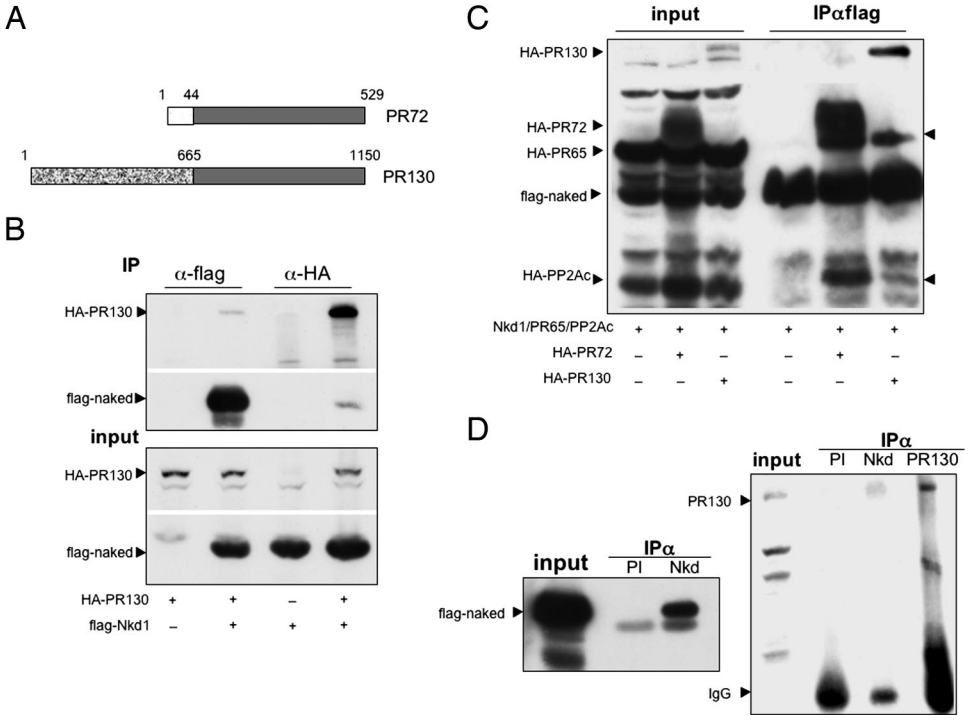

Fig. 1. PR130 can interact with Nkd. (*A*) PR72 has an N-terminal stretch of 44 specific amino acids (light speckled), whereas PR130 has a 665-N-terminal-specific stretch (dark speckled). (*B*) IP of PR130 and Nkd. Extracts from HEK 293 ectopically expressing flag-tagged hNkd1, HA-tagged hPR130, or both were subjected to co-IP with anti-flag and anti-HA antibodies as indicated. Flag-antibodies did not precipitate HA-PR130 (lane 1), and the HA-antibody did not precipitate flag-hNkd1 (lane 3); when coexpressed, both were coprecipitated with either anti-HA or ant-flag (lanes 2 and 4). (*Lower*) Shown is 10% of the input in either lane. (*C*) IP of PR130 and Nkd containing the PP2A holoenzyme. Extracts from HEK 293 cells expressing flag-Nkd1, HA-PP2Ac, and HA-PR65 (input, *Left*) were cotransfected with either HA-PR72 (lane 2) or HA-PR130 (lane 3). IP anti-flag (*Right*) pulled down flag-Nkd1 (lane 1). PP2Ac and PR65 were pulled down only in the presence of PR72 (lane 2) or PR130 (lane 3) indicated with arrowheads. (*D*) IP of endogenous PR130 using an anti-Nkd antibody able to precipitate flag-Nkd1 (*Left*). PI, preimmune serum. (*Right*) IP on U2OS lysate using PI, anti-Nkd, or anti-PR130 antibody. PR130 is shown by arrowhead.

we reasoned that a functional similarity might exist between these two variants. We therefore asked whether PR130, like PR72, was also able to interact with Nkd in coimmunoprecipitation (co-IP) assays. We generated a hemagglutinin (HA)-tagged expression construct for PR130 and found that, when coexpressed with flag-tagged human Naked cuticle (hNkd1) in human embryonic kidney (HEK) 293 cells, HA-PR130 was detected in an anti-flag-IP (Fig. 1*B*). No PR130 was detected in the absence of flag-hNkd1, indicating that PR130 can specifically interact with Nkd (Fig. 1*B*). The reverse IP using anti-HA to pull down PR130 shows detection of flag-hNkd1 in the presence of HA-PR130, but not in the absence of HA-PR130, further confirming that these two proteins can interact. PR72 and PR130 were earlier identified as PP2A regulatory subunits, which are proposed to function as targeting proteins that direct the phosphatase holoenzyme to specific substrates (20). We therefore asked whether PR130 was able to recruit the complete PP2A holoenzyme (consisting of the catalytic subunit PP2Ac and the structural subunit PR65) to Nkd. Co-IP assays with hNkd1 show that both PR72 and PR130 interact with Nkd, and the PP2A holoenzyme complex components PR65 and PP2Ac are also coimmunoprecipitated (Fig. 1*C*). Because PP2Ac and PR65 were found associated with Nkd only when either PR72 or PR130 was present, we conclude that both proteins are able to bind hNkd1 and recruit the PP2A holoenzyme. We next wanted to confirm the interaction between PR130 and Naked in endogenous complexes. We used an antibody raised against two hNkd1-specific peptides and found that this antibody was able to pull down flag-Nkd1 from cell lysates (Fig. 1*D Left*). The antibody was not able to detect denatured Nkd in cell lysates on Western blot. We used this antibody to perform co-IP assays on U2OS cell lysates expressing ectopic Wnt-1 and stained on Western blot with an anti-PR130 antibody. We could pull down PR130 (Fig. 1*D Right*) with the anti-Nkd antibody, but not with preimmune serum (PI). Together, these data suggest that PR130 and Nkd can form a physical complex *in vivo*.

PR130 Is a Positive Regulator of the Canonical Wnt-Signaling Pathway. Based on the physical interaction data, one would predict that both PR72 and PR130 function as regulators of Wnt signaling. To test this prediction, we evaluated the activity of a Wnt-responsive Top-Glow luciferase reporter construct in HEK 293 cells. We found that ectopic PR130 expression activates the TOP-Glow reporter (Fig. 2*A*) but not the FOP-Glow reporter containing mutated TCF sites (data not shown). This result is unlike PR72, which inhibits reporter activity, as reported (19). To investigate this finding further, we generated two distinct short-hairpin RNA (shRNA) knockdown vectors targeting endogenous PR130 for suppression. We tested both vectors functionally using cotransfection of HA-PR130 and evaluating protein levels on Western blot (Fig. 2*B Lower*) and using quantitative RT-PCR (QRT-PCR) on endogenous PR130 RNA (Fig. 2*B Upper*). We found that both our shRNAs targeted ectopic and endogenous PR130 for suppression. We then tested our shRNA vectors for activity on a Top-Glow reporter and found that both were able to reduce its activity (Fig. 2*C*), suggesting that endogenous PR130 functions to enhance Wnt signaling. Additionally, we found that, in cells that have lost PR72 because of shRNA-mediated suppression, PR130 is a more potent activator of the Wnt-signaling pathway, consistent with the notion that both proteins act in the same pathway (Fig. 2*D*). These combined results indicate that PR130 is a positive regulator of Wnt signaling in cell culture. Because PR72 overexpression is associated with loss of dishevelled stability, we asked whether PR130 could then function to stabilize dishevelled. We could, however, not find a significant stabilization of dishevelled levels (Fig. 2*E*). We then analyzed the interaction between Nkd and dishevelled in the presence of ectopic PR130 and found that this interaction was reduced (Fig. 2*E*). Losing the interaction between dishevelled and its negative regulator Nkd could at least in part account for the positive effect of PR130 observed on the Wnt-signaling cascade.

PR130 Is Required for Proper Organization of Somites During Embryonic Development. Based on the findings above, we asked whether PR130 is a positive modulator of the Wnt pathway during early vertebrate development. We identified the EST coding for the 5′ sequence of *Xenopus PR130* (*Xpr130*) from the Department of Energy Joint Genome Institute (JGI) *Xenopus tropicalis* database (www.jgi.doe.gov) and generated primers to evaluate expression of X*PR130* by RT-PCR at different embryonic stages of development

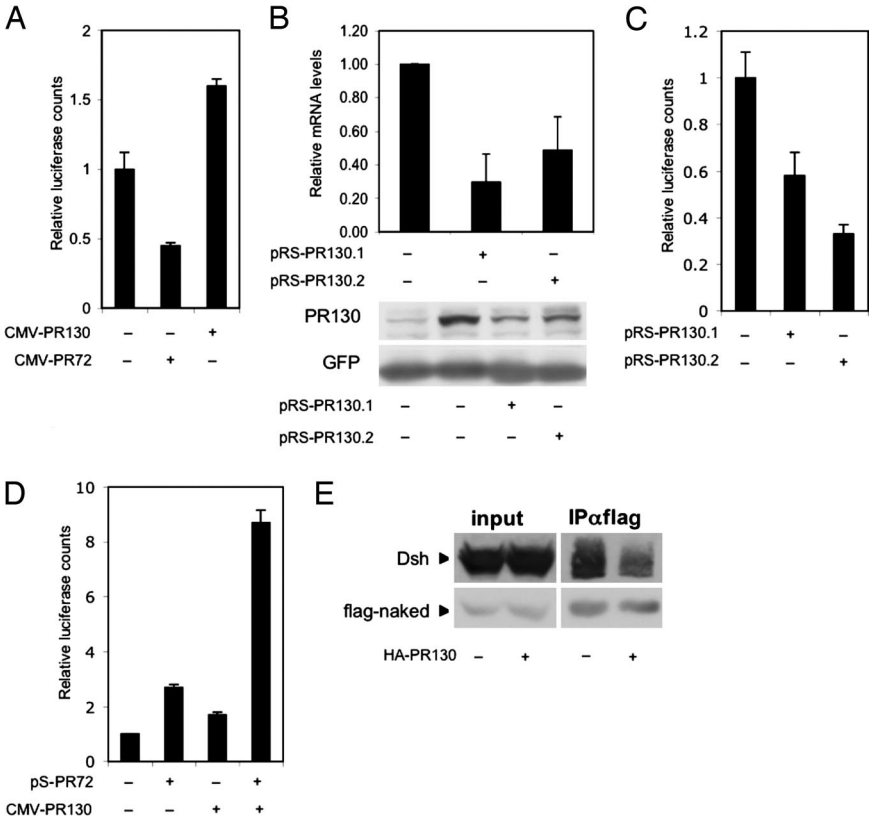

Fig. 2. PR130 is an activator of the classical Wnt-signaling pathway. TCF containing Top-Glow or Fop-Glow (containing mutated TCF sites) luciferase reporter, CMV *Renilla* luciferase, and Wnt-1 was cotransfected in HEK 293 cells (*A*) with or without HA-PR72 or HA-PR130 as indicated (*C*) or with pS-PR72 or pRS-PR130. The bars represent relative luciferase activity compared with the first bar in the graph. (*B Lower*) Western blot showing extracts from HEK 293 cells coexpressing HA-PR130 (lanes 2–4) and GFP (all lanes) as a loading control. pRS-PR130.1 (lane 3), pRS-PR130.2 (lane 4), or pRS (lanes 1 and 2) was cotransfected. (*B Upper*) QRT-PCR showing relative amount of mRNA levels of endogenous PR130 in the presence of indicated PR130 targeting pRetroSuper vectors or a control vector. (*D*) Top-Glow reporter assay as described for Fig. 2 *A* and *C* with either pS-PR72 or CMV HA-PR130 or a combination of the two as indicated. (*E*) IP of flag-Naked pulling down dishevelled in the presence (lane 4) or absence (lane 3) of ectopic PR130. Lanes 1 and 2 show the corresponding inputs.

in *X. tropicalis*. We found that *Xpr130*, like *Xpr72*, is maternally expressed and present during all stages of early embryonic development (Fig. 3*A*). Whole-mount *in situ* hybridization (ISH) revealed specific expression of *Xpr130* in the paraxial mesoderm and the somites of neurula and tailbud stage embryos (Fig. 3*A Lower*) similar to that of *Xpr72* (ref. 19 and data not shown). At the tailbud stage, *Xnaked* is also restricted to somites (Fig. 3*B*). Next, we wished to investigate the effect of loss of Xpr130 on *Xenopus* embryonic development. Depletion of Xpr130 by injection of two-cell stage embryos with Xpr130 morpholino oligonucleotides (MO) resulted in embryos with an underdeveloped tail and affected somites (Fig. 3 *C Right* and *D Center*).

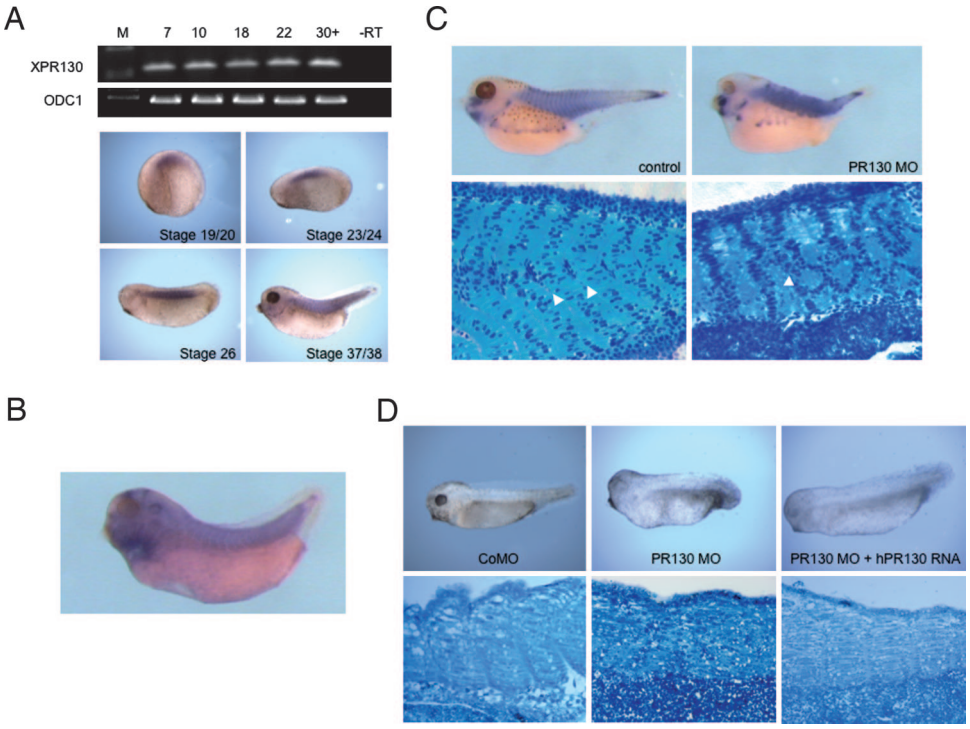

Fig. 3. PR130 depletion affects somite organization and tail development. (*A*) RT-PCR analysis of *X. tropicalis* total RNA from different developmental stages. Xpr130 is expressed maternally (stage 7) and throughout early development (stages 10, 18, 22, and 30). −RT, RT-PCR without reverse transcriptase. ODC1 expression was used as loading control. (*A Lower*) Whole-mount ISH for Xpr130 in embryos showing predominant staining of somites from the earliest stage detectable. (*B*) ISH of tailbud stage embryo with an Xnkd-specific probe. (*C*) Control embryo shows organized somites in a chevron-like shape as visualized by whole-mount ISH by using XmyoD as a marker (*Left*). PR130-depleted embryos lack chevron-like shaped somites (*Right*). Arrowheads show somitic borders. (*D*) Similar to *B* but without XmyoD. Shown are embryos injected with control MO (CoMO) (*Left*), PR130 MO (*Center*), and PR130 MO plus hPR130 RNA (*Right*). (*Lower*) Sagittal sections of the somites.

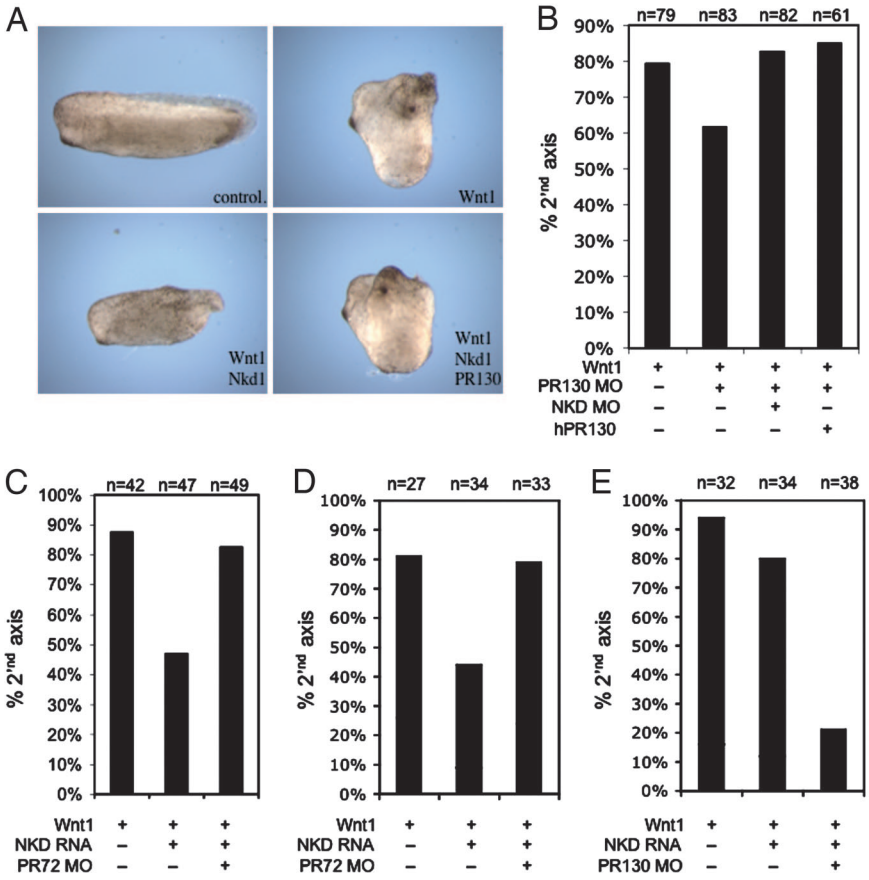

Fig. 4. PR130 depletion enhances the inhibitory function of Nkd on the Wnt-signaling cascade. (*A*) Embryos shown as representative for *C* injected as indicated. (*B*) PR130 depletion inhibits the ectopic Wnt signal but not in the absence of Nkd. The effect is also rescued by add-back of ectopic hPR130. (*C*) Nkd antagonizes an ectopic Wnt signal but not in the presence of ectopic PR130. (*D*) Loss of PR72 abrogates Naked-mediated inhibition of the Wnt signal. (*E*) In contrast, injection of suboptimal amounts of Nkd RNA demonstrates that loss of PR130 enhances the antagonizing function of Nkd.

Because PR130, like PR72 and Nkd, is expressed in the somites of embryos, we analyzed the formation of the somites in the absence of PR130, using ISH with XmyoD as a marker (Fig 3*C*) of methylene blue staining (Fig. 3*D*). We found that, when Xpr130 was depleted, segmentation still occurred, but the somites lost their characteristic chevron-like shape, as seen in control embryos (Fig. 3 *C Right* and *D Center*). Moreover, their strict position toward each other was also disturbed. We analyzed this phenotype in more detail by sectioning the embryos and found strong disorganization within the somites. Somite boundaries were not organized in parallel to each other but seemed to be positioned rather randomly from dorsal to ventral (Fig. 3*C Lower* arrowheads). Cells within the somites were also disorganized, sometimes forming circular structures. When we injected control MO (random sequences; Gene Tools, Philomath, OR), development of the tail was not affected and somite boundaries were normal (Fig. 3*D Left*). To test the morpholino specificity, we restored PR130 levels in the embryo by coinjecting hPR130 RNA. This add-back experiment rescued both the developmental defects in the somites and the defects in tail development caused by PR130 depletion (Fig. 3*D Right*). This result demonstrates that Xpr130 is required for the proper structural organization of somites and the proper development of the tail during embryogenesis.

PR130 Depletion Abrogates Ectopic Wnt Activity in *Xenopus* Embryos. To further study the effects of Xpr130 on the Wnt-signaling pathway *in vivo*, we used the Wnt-induced secondary body axis assay (21) in *X. tropicalis*. *Wnt-1* RNA and control MO (CoMO) were injected in ventral blastomeres of four-cell-stage *Xenopus* embryos to induce a secondary body axis (Fig. 4*A Upper*). When we coinjected PR130 MO, the formation of a secondary body axis by Wnt1 was repressed, suggesting that Xpr130 is required for the proper transduction of the Wnt signal (Fig. 4*B*). Restoring PR130 levels by coinjecting hPR130 RNA clearly rescued the effect of PR130 depletion on Wnt-1 signal transduction in the *Xenopus* embryo (Fig. 4*B*), demonstrating that the effects observed were due to loss of Xpr130. This finding confirms the results in tissue culture, which also suggested that PR130 is a positive regulator of canonical Wnt signaling. Because PR130 interacts with Nkd, PR130 may not function directly as a positive regulator of the Wnt-signaling pathway, but rather functions by affecting Nkd as a Wnt antagonist. To test this hypothesis, we depleted *Xenopus* Nkd (Xnkd) by coinjecting Xnkd MO and found that Wnt-1-mediated second axis induction, disturbed by loss of PR130, was restored to normal (Fig. 4*B*). Thus, Xpr130 seems to depend on the presence of Xnkd to mediate its effects on the Wnt-signaling pathway.

PR130 Prevents Nkd/PR72-Mediated Repression of the Wnt-Signaling Pathway. To further address whether the repressive function of Xnkd on the canonical Wnt-signaling pathway is indeed affected by Xpr130, we repeated the Wnt-1-induced secondary body axis assay in the presence of *hNkd1* RNA to antagonize the formation of the secondary body axis (Fig. 4 *C* and *A Lower Left*). Coinjection of *hPR130* RNA strongly inhibited the antagonizing effect of Nkd on the Wnt-signaling pathway, resulting in an increased number of embryos with a secondary body axis (Fig. 4 *C* and *A Lower Right*). This finding suggests that PR130 is indeed a negative regulator of Nkd function and demonstrates opposing activities of PR72 and PR130 on the ability of Nkd to restrict Wnt signaling. In support of this notion, we find that *hNkd1* mRNA (suboptimal amounts for Wnt repression) is a better antagonist of Wnt1-induced second body axis in the absence of PR130 (Fig. 4*E*), which is again opposite to what was found for loss of PR72 (Fig. 4D and ref. 19). Together, these results suggest that Nkd function is fine-tuned by a molecular mechanism in which the inhibitory activity of Nkd/PR72 on Wnt signaling can be antagonized by Nkd/PR130.

Discussion

Nkd was the first-described Wnt-inducible antagonist of the Wnt pathway, thus establishing a negative feedback loop to restrict the Wnt signal (14). Besides its binding to dishevelled (18) and its proposed dependence on PR72 for repression (19), not much is known about the mechanism underlying the Wnt-inhibitory function of this protein. Here, we describe PR130, a proposed PP2A regulatory B-subunit (20), as a modulator of the Wnt-signaling cascade. We show that PR130 can bind to Nkd and recruit the PP2A holoenzyme. When studying the effect of PR130 on the Wnt-signaling pathway, we find opposing activities of PR72 and PR130. Cell-based Wnt reporter assays indicate that PR130 is an activator of Wnt signaling, whereas our previous data indicate that PR72 acts as a repressor of Wnt signaling (19). The effects of PR130 on Wnt signaling, observed in cell-based assays, was further confirmed by experiments in *Xenopus* embryos, where we show that PR130 depletion abolishes activation of the Wnt pathway. This effect depends on Nkd, because it is rescued by coinjection of an Xnkd targeting MO. This finding would suggest that PR130 activates Wnt signaling by inhibiting the function of Nkd. Two sets of experiments using second axis formation in *Xenopus* development support this notion. First, Naked is a better inhibitor of Wnt signaling in the absence of PR130. Second, ectopic PR130 can repress Naked-mediated inhibition of the Wnt signal. These results demonstrate that PR130 enhances Wnt signaling, most likely by limiting the effects of Nkd.

Although PR130, PR72, and Nkd RNA levels are maternally present, depletion of neither one of them seemed to affect early Wnt signaling, which is known to be required for setting up the embryonic body axis (22). This finding could suggest that transduction of the earliest endogenous Wnt signal is independent of the presence of PR130 (PR72 and Nkd). Another possibility is that MO-mediated gene targeting is not efficient enough to deplete the maternal contribution of PR130 to affect the Wnt signal. Consistent with this finding, when very high amounts of Wnt RNA were used to ectopically induce second body axis formation, we found that modulation of the signal by any of our MOs is no longer possible (data not shown).

We find that absence of *Xenopus* PR130 during early development causes a deregulation in tail development. Because development of the tail requires Wnt signaling (23), the phenotype of Xpr130 knockdown might be explained by inhibition of Wnt signaling during development. Similarly, development of the tail was found to be impaired when Wnt signaling was inhibited in zebrafish (24). However, we cannot exclude any Wnt-independent effects on growth in general. Although PR72 depletion caused complete lack of eye development, which is similar to zebrafish mutants with ectopic Wnt (25), PR130-depleted embryos did not show gross defects in eye differentiation, which is not surprising because Wnt signaling needs to be inactive for the development of anterior structures such as the eye (25).

Additionally, we found that Xpr130-depleted embryos display disturbed somite organization. A role for Wnt signaling in segmentation and somitogenesis has been described earlier (3, 26). Also, Lef1 mutant mice demonstrate a function for Lef1 in somitogenesis, because these mutant mice show a lack of segmented somites (27). We found previously that, in PR72-depleted embryos, the somites were smaller compared with noninjected embryos. PR130-depleted embryos show different defects. Rather than the size of the somites, we find that the structural organization is lost although somite boundaries are still formed. These results further support the requirement of tight control of the Wnt-signaling cascade during patterning and somitogenesis.

We have shown previously that ectopic expression of PR72 causes proteasome-mediated destruction of dishevelled (19). When we evaluated the levels of dishevelled in cells expressing ectopic PR130, we saw no significant effects on dishevelled stability. It is possible that PR130 regulates a specific pool of dishevelled, which is small compared with total dishevelled and therefore remains below our detection limit. Alternatively, it is equally possible that regulation of dishevelled stability, as observed for PR72, is causally unrelated to its ability to modulate the Wnt-signaling cascade, but rather a consequence of Naked/PR72-mediated Wnt inhibition. We did find that, when ectopically expressed, PR130 can disrupt binding between dishevelled and Nkd, which could account for its ability to activate Wnt signaling. How this disruption translates into a more active Wnt signal requires a complete understanding of the mechanism behind Nkd-mediated regulation of Wnt signaling, which is still elusive.

Both PR72 and PR130 are proposed to function as PP2A regulatory B-subunits that target the PP2A holoenzyme to a substrate. We have no indications from phosphate labeling or gel electrophoresis experiments that Nkd itself or dishevelled is a target for PR72- or PR130-mediated dephosphorylation (data not shown). However, it is possible that a single regulatory site on Nkd is modulated, which would not show up on assays evaluating total protein phosphorylation. Alternatively, a third yet unidentified, Nkd-interacting protein involved in regulating the function of Nkd, might be targeted by these proteins. A third and more intriguing possibility is that these subunits do not function to target the PP2A holoenzyme to a substrate, but are themselves targets of PP2A. In support of this idea, we have found that PR72 can be phosphorylated by treating cells with okadaic acid, a chemical inhibitor of PP2A (data not shown). It is, however, difficult to establish whether this phosphorylation represents a lack of dephosphorylation or the activation of a PP2A-regulated kinase. Future experiments will have to establish the exact molecular role of PR72 and PR130 in modulating the antagonistic function of Nkd.

Others have previously shown that other PP2A B-subunits are also involved in modulation of the Wnt-signaling pathway (28–31). These results and ours illustrate the dynamic interaction of the PP2A holoenzyme with the Wnt-signaling cascade at different levels and underscore the importance of investigating separate holoenzyme complexes rather than general PP2A activity. PR72 and PR130 are generated by initiation of transcription from distinct promoters to generate two proteins having a common C terminus and distinct N termini (20). It will be of interest to study the promoters that generate these two structurally related, but functionally antagonistic, proteins in more detail. We have found no evidence that PR72 and PR130 themselves are transcriptional targets of the Wnt-signaling cascade (data not shown), which is not surprising because they both depend on the Wnt target Nkd for modulation of Wnt signaling. The identification of PR130 as a new modulator of the Wnt-signaling cascade and its opposing effects on Nkd function compared with PR72 add a new level of complexity, allowing the cell to fine-tune the effect of Nkd on Wnt signaling.

Materials and Methods

Manipulation of *X. tropicalis* Embryos. *X. tropicalis* embryos were obtained by natural mating (as described by R. Grainger at http://faculty.virginia.edu/xtropicalis/). Plasmid DNA of T7Ts-XWnt-1 (32), T7Ts-hNkd, and T7Ts-hPR130 were linearized and used as template for synthesis of capped mRNA by using MESSAGE MACHINE (Ambion, Austin, TX). Capped mRNA transcripts were purified by using RNeasy columns (Qiagen, Valencia, CA).

Embryos were injected at the four-cell stage in both ventral blastomeres with Wnt-1 RNA (0.5 pg) and coinjected with Nkd RNA (8 pg) alone or in combination with control MO (10 ng), PR130 (10 ng), or PR72 MO (10 ng) (Gene Tools). For MO injections alone, 10 or 20 ng of three nonoverlapping MO was injected at the two-cell stage in both blastomeres. All experiments were done at least three times to ensure specific effects of MO and RNA injections. Representative experiments are shown. After injection, embryos were raised at 23°C in a standard amphibian saline solution [12% modified Marc's Ringer's solution (MMR)]

with the addition of 3% Ficoll in the first 6 h (Amersham Pharmacia Biosciences). At the appropriate stages, embryos were fixed in MEMPFA [100 mM Mops (Sigma), pH 7.4/2 mM EGTA (Sigma)/1 mM $MgSO_4$ (Merck)/4% paraformaldehyde (Sigma)]. Embryos were staged according to ref. 33.

Whole-Mount ISH. Whole-mount ISH were performed as described (34), with hybridization at 65°C and RNase treatment. All ISH experiments were performed four times with four to five embryos. Sense probe did not stain these embryos. Probes used were as follows: XmyoD (35) PR130 and Nkd probes were generated by RT-PCR from total RNA of *X. tropicalis* embryos. Primers were generated by using the *X. tropicalis* EST database (Sanger Institute, Cambridge, U.K.). PCR fragments were cloned in pGEM-T easy (Promega) and analyzed by sequencing. DNA plasmids were linearized and used as template for digoxigenin (DIG)-labeled antisense RNA synthesis (Roche Diagnostics). RNA probes were purified by using RNeasy columns (Qiagen).

Cell Lines, Transfections, and Luciferase Assays. HEK 293 cells were cultured in DMEM supplemented with 10% FCS, L-glutamine, and penicillin/streptomycin (GIBCO). Transient transfections in these cells were performed by the calcium phosphate precipitation method (36). Luciferase assays were performed by using the Dual luciferase system (Promega). One hundred nanograms of Top-Glow or Fop-Glow luciferase vector was transfected in the presence of 5 ng of CMV-Wnt1 and 20 ng of CMV *Renilla* luciferase. For loss-of-function assays, 2 μg of either pSUPER or pRETRO-SUPER (37) was cotransfected, and luciferase counts were measures 48–72 h after transfection on the TD-20/20 luminocounter (Promega). For gain-of-function assays, 500 ng of CMV construct was cotransfected, and luciferase counts were measured 24–48 h after transfection.

Plasmids and Reagents. Anti-flag (m2) was purchased from Sigma, and anti HA (Y11), anti-GFP (FL), and anti Dsh (3F12, 10B5, and 4D3) antibodies were purchased from Santa Cruz Biotechnology. The PR130 cDNA and the rabbit anti-PR130 antiserum (raised against ^{1143}KLQSVDEE^{1150}) were a gift from B. Hemmings. Rabbit antiserum raised against Naked specific peptides SELPPRTSNPTRSRSH and RLRGTQDGSKHFVRS was bought from Eurogentech (Brussels). PR130 was digested as an EcoRV/BamHI fragment from pBSK-PR130 (20) and ligated into the EcoRV/BamHI sites of pMV (38). CMV-HA-PR130 was cloned as a BamHI/XhoI fragment from pMV-HA-PR130 and ligated into pcDNA.1(−) (Invitrogen). CMV-HA-PR72, CMV-HA-PP2Ac, CMV-HA-PR65, and flag-hNkd1 have been described (19). Top- and Fop-Glow reporter constructs were a gift from H. Clevers, and 19-mer hairpin oligos for hPR130 #1(GCACATCCCTGTGTCTCAG) and #2(CAGTAGCCAGGAAGAGATA) were cloned into pRETRO-SUPER as described (25). Morpholino antisense oligos targeting XPR130 (1: CCTTGTAAGGTGCAGCCATCTGGCC, 2: TAAATTAAATCAAAGAAGACTGCCC, 3: TAAAGGTCAGCACTGATCCAACAGT) were bought from Gene Tools. For the T7T6-hPR130 expression construct, hPR130 was cut as a BamHI/EcoRV fragment from pCMV-HA-PR130, blunted with klenow, and cloned into the EcoRV site of T7T6 vector in between the 5′ and 3′ β-globin UTR.

QRT-PCR. QRT-PCR was performed on an ABI Prism 7000 Sequence Detection System (Applied Biosystems) by using SYBR Green Master Mix (4309155, Applied Biosystems) according to the manufacturer's protocol. Primers used were as follows: 5′-GGCAACGAGGTTTCTCTGTCA-3′ and 5′-AAGTATTGTGATAACTGAGTCCTCCAAA-3′ for PR130.

Immunoblotting and Co-IP Experiments. Cells were lysed in 0.5 ml of NETN lysis buffer (100 mM NaCl/1 mM EDTA/20 mM Tris, pH 8.0/0.5% Nonidet P-40) containing complete protease inhibitor mixture (Roche Diagnostics), 10 mM NaF, and 10 mM β-glycerolphosphate, and complexes were immunoprecipitated with 2 μg of the indicated antibody, preconjugated to protein G Sepharose beads. After three wash steps in lysis buffer, bound proteins were eluted by boiling in SDS-sample buffer and resolved by SDS/PAGE. Western blots were performed by using whole-cell extracts, separated on 6–10% SDS/PAGE gels and transferred to poly(vinylidine difluoride) membranes (Millipore).

We thank Hans Clevers (Hubrecht Laboratory, Utrecht, The Netherlands) and Brian Hemmings (Friedrich Miescher Institute, Basel, Switzerland) for the kind gift of reagents and plasmids and Drs. Sebastian Nijman and Helen Pickersgrill for critical reading of the manuscript. This work was supported by European Union Grant QLRT-2000-01275 (to G.R.) and a grant from the Dutch Cancer Society.

1. Moon, R. T. & Kimelman, D. (1998) *BioEssays* **20,** 536–545.
2. Keller, R. (2002) *Science* **298,** 1950–1954.
3. Aulehla, A. & Herrmann, B. G. (2004) *Genes Dev*. **18,** 2060–2067.
4. Zhu, A. J. & Scott, M. P. (2004) *Genes Dev*. **18,** 2985–2997.
5. Logan, C. Y. & Nusse, R. (2004) *Annu. Rev. Cell Dev. Biol*. **20,** 781–810.
6. Wharton, K. A., Jr. (2003) *Dev. Biol*. **253,** 1–17.
7. Boutros, M. & Mlodzik, M. (1999) *Mech. Dev*. **83,** 27–37.
8. Amit, S., Hatzubai, A., Birman, Y., Andersen, J. S., Ben-Shushan, E., Mann, M., Ben-Neriah, Y. & Alkalay, I. (2002) *Genes Dev*. **16,** 1066–1076.
9. van de Wetering, M., Cavallo, R., Dooijes, D., van Beest, M., van Es, J., Loureiro, J., Ypma, A., Hursh, D., Jones, T., Bejsovec, A., *et al*. (1997) *Cell* **88,** 789–799.
10. Giles, R. H., van Es, J. H. & Clevers, H. (2003) *Biochim. Biophys. Acta* **1653,** 1–24.
11. Polakis, P. (2000) *Genes Dev*. **14,** 1837–1851.
12. Jho, E. H., Zhang, T., Domon, C., Joo, C. K., Freund, J. N. & Costantini, F. (2002) *Mol. Cell. Biol*. **22,** 1172–1183.
13. Lustig, B., Jerchow, B., Sachs, M., Weiler, S., Pietsch, T., Karsten, U., van de Wetering, M., Clevers, H., Schlag, P. M., Birchmeier, W. & Behrens, J. (2002) *Mol. Cell. Biol*. **22,** 1184–1193.
14. Zeng, W., Wharton, K. A., Jr., Mack, J. A., Wang, K., Gadbaw, M., Suyama, K., Klein, P. S. & Scott, M. P. (2000) *Nature* **403,** 789–795.
15. Noordermeer, J., Johnston, P., Rijsewijk, F., Nusse, R. & Lawrence, P. A. (1992) *Development (Cambridge, U.K.)* **116,** 711–719.
16. Wharton, K. A., Jr., Zimmermann, G., Rousset, R. & Scott, M. P. (2001) *Dev. Biol*. **234,** 93–106.
17. Yan, D., Wallingford, J. B., Sun, T. Q., Nelson, A. M., Sakanaka, C., Reinhard, C., Harland, R. M., Fantl, W. J. & Williams, L. T. (2001) *Proc. Natl. Acad. Sci. USA* **98,** 3802–3807.
18. Rousset, R., Mack, J. A., Wharton, K. A., Jr., Axelrod, J. D., Cadigan, K. M., Fish, M. P., Nusse, R. & Scott, M. P. (2001) *Genes Dev*. **15,** 658–671.
19. Creyghton, M. P., Roel, G., Eichhorn, P. J., Hijmans, E. M., Maurer, I., Destree, O. & Bernards, R. (2005) *Genes Dev*. **19,** 376–386.
20. Hendrix, P., Mayer-Jackel, R. E., Cron, P., Goris, J., Hofsteenge, J., Merlevede, W. & Hemmings, B. A. (1993) *J. Biol. Chem*. **268,** 15267–15276.
21. McMahon, A. P. & Moon, R. T. (1989) *Cell* **58,** 1075–1084.
22. Tao, Q., Yokota, C., Puck, H., Kofron, M., Birsoy, B., Yan, D., Asashima, M., Wylie, C. C., Lin, X. & Heasman, J. (2005) *Cell* **120,** 857–871.
23. Agathon, A., Thisse, C. & Thisse, B. (2003) *Nature* **424,** 448–452.
24. Thorpe, C. J., Weidinger, G. & Moon, R. T. (2005) *Development (Cambridge, U.K.)* **132,** 1763–1772.
25. van de Water, S., van de Wetering, M., Joore, J., Esseling, J., Bink, R., Clevers, H. & Zivkovic, D. (2001) *Development (Cambridge, U.K.)* **128,** 3877–3888.
26. Linker, C., Lesbros, C., Gros, J., Burrus, L. W., Rawls, A. & Marcelle, C. (2005) *Development (Cambridge, U.K.)* **132,** 3895–3905.
27. Galceran, J., Sustmann, C., Hsu, S. C., Folberth, S. & Grosschedl, R. (2004) *Genes Dev*. **18,** 2718–2723.
28. Li, X., Yost, H. J., Virshup, D. M. & Seeling, J. M. (2001) *EMBO J*. **20,** 4122–4131.
29. Seeling, J. M., Miller, J. R., Gil, R., Moon, R. T., White, R. & Virshup, D. M. (1999) *Science* **283,** 2089–2091.
30. Yang, J., Wu, J., Tan, C. & Klein, P. S. (2003) *Development (Cambridge, U.K.)* **130,** 5569–5578.
31. Bajpai, R., Makhijani, K., Rao, P. R. & Shashidhara, L. S. (2004) *Development (Cambridge, U.K.)* **131,** 1007–1016.
32. Noordermeer, J., Meijlink, F., Verrijzer, P., Rijsewijk, F. & Destree, O. (1989) *Nucleic Acids Res*. **17,** 11–18.
33. Nieuwkoop, P. D. & Faber, J. (1967) *Normal Table of Xenopus laevis (Daudin)* (North-Holland Publishing Co., Amsterdam), 2nd Ed.
34. Harland, R. M. (1991) *Methods Cell Biol*. **36,** 685–695.
35. Roel, G., Hamilton, F. S., Gent, Y., Bain, A. A., Destree, O. & Hoppler, S. (2002) *Curr. Biol*. **12,** 1941–1945.
36. van der Eb, A. J. & Graham, F. L. (1980) *Methods Enzymol*. **65,** 826–839.
37. Brummelkamp, T. R., Bernards, R. & Agami, R. (2002) *Science* **296,** 550–553.
38. Voorhoeve, P. M., Hijmans, E. M. & Bernards, R. (1999) *Oncogene* **18,** 515–524.